Homo- and heteromeric assembly of TRPV channel subunits

Nicole Hellwig, Nadine Albrecht, Christian Harteneck, Günter Schultz and Michael Schaefer*

Institut für Pharmakologie, Charité-Universitätsmedizin Berlin, Campus Benjamin Franklin, Thielallee 67-73, 14195 Berlin, Germany

*Author for correspondence (e-mail: schae@zedat.fu-berlin.de)

Accepted 6 December 2004
Journal of Cell Science 118, 917-928 Published by The Company of Biologists 2005
doi:10.1242/jcs.01675

Summary

The vanilloid receptor-related TRP channels (TRPV1-6) mediate thermosensation, pain perception and epithelial Ca^{2+} entry. As the specificity of TRPV channel heteromerization and determinants governing the assembly of TRPV subunits were largely elusive, we investigated the TRPV homo- and heteromultimerization. To analyze the assembly of TRPV subunits in living cells, we generated fluorescent fusion proteins or FLAG-tagged TRPV channel subunits. The interaction between TRPV subunits was assessed by analysis of the subcellular colocalization, fluorescence resonance energy transfer and coimmunoprecipitation. Our results demonstrate that TRPV channel subunits do not combine arbitrarily. With the exception of TRPV5 and TRPV6, TRPV channel subunits preferentially assemble into homomeric complexes. Truncation of TRPV1, expression of cytosolic termini of TRPV1 or TRPV4 and construction of chimeric TRPV channel subunits revealed that the specificity and the affinity of the subunit interaction is synergistically provided by interaction modules located in the transmembrane domains and in the cytosolic termini. The relative contribution of intramolecularly linked interaction modules presumably controls the overall affinity and the specificity of TRPV channel assembly.

Supplementary material available online at
http://jcs.biologists.org/cgi/content/full/118/5/917/DC1

Key words: Vanilloid receptors, Transient receptor potential channel, Multimerization, Hetero-oligomeric quaternary structure, Epithelial calcium channels

Introduction

Transient receptor potential (TRP) channels are members of the superfamily of hexahelical cation channels. Like voltage-gated K^+ channels (Roosild et al., 2004), inwardly rectifying K^+ channels (Bichet et al., 2003), cyclic nucleotide-gated (CNG) channels (Kaupp and Seifert, 2002) or hyperpolarization-activated and cyclic nucleotide-regulated (HCN) channels (Zagotta et al., 2003; Robinson and Siegelbaum, 2003), TRP channel subunits presumably assemble into homo- or heterotetrameric channel complexes. The subunit composition may influence the biophysical and regulatory properties of the resulting channel complex. Hetero-oligomeric TRP channel complexes were first demonstrated between the eye-specific TRP channel subunits TRP and TRP-like (TRPL) in *Drosophila melanogaster* and result in cation currents with unique permeation properties and low constitutive activity (Xu et al., 1997). Additionally, TRPL may also assemble with TRPγ to form a phospholipase C-stimulated channel (Xu et al., 2000). In mammals, various heteromeric TRPC channel complexes can be formed including heteromers of TRPC1, TRPC4 and TRPC5 (Goel et al., 2002; Hofmann et al., 2002; Strübing et al., 2001) or of TRPC3, TRPC6 and TRPC7 (Hofmann et al., 2002; Goel et al., 2002). An assembly of TRPC1 and TRPC3 has been demonstrated (Xu et al., 1997), but could not be confirmed in other studies (Hofmann et al., 2002; Goel et al., 2002).

The vanilloid receptor TRPV1 was the founding member of the TRPV channel family (Caterina et al., 1997), which consists of six mammalian members TRPV1-TRPV6 (Gunthorpe et al., 2002; Peng et al., 2001). Homo-oligomeric TRPV1-TRPV4 channels form poorly selective cation channels that are sensitive to heat (Caterina et al., 1997; Caterina et al., 1999; Smith et al., 2002; Watanabe et al., 2002b) and are additionally regulated by protons (TRPV1) and various lipid mediators including the TRPV1-activating chilli pepper constituent capsaicin (Caterina et al., 1997) or TRPV4-activating 4α-phorbol esters (Watanabe et al., 2002a). Recently, the stimulation of TRPV4 by hypotonic extracellular solutions (Strotmann et al., 2000) has been shown to be mediated by formation of arachidonic acid and its metabolites including the TRPV4-activating messenger 5′,6′-epoxyeicosatrienoic acid (Vriens et al., 2004). TRPV5 and TRPV6 are phylogenetically closely related Ca^{2+}-selective channels expressed in epithelia of intestine and kidney (den Dekker et al., 2003). Furthermore, both channels exhibit a constitutive activity and are transcriptionally regulated by 1α,25-dihydroxycholecalciferol. TRPV1, TRPV5 and TRPV6 have been shown to assemble into tetrameric complexes (Kedei et al., 2001; Hoenderop et al., 2003). A hetero-oligomer formation between TRPV channel subunits has been proposed for TRPV1 and TRPV3 (Smith et al., 2002) as well as for TRPV5 and TRPV6 (Hoenderop et al., 2003). A systematic and combinatorial analysis of TRPV homo- and hetero-oligomerization, however, is lacking. Moreover, structural

determinants that contribute to the affinity and selectivity of the subunit assembly are largely unknown.

We studied the selectivity and promiscuity of homo- and heteromultimerization between TRPV channel subunits in living cells. By analyzing the colocalization, fluorescence resonance energy transfer (FRET) and coimmunoprecipitation of TRPV1-TRPV6 we show here that the formation of homo-oligomeric channel complexes is favored by most members of the TRPV family. The analysis of the contribution of cytosolic N- and C-termini as well as of the transmembrane domains suggests a complex mechanism of channel assembly. Experimental data support a model in which both cytosolic domains and the transmembrane domain of TRPV channel subunits synergistically contribute to the overall affinity and selectivity of TRPV channel assembly.

Materials and Methods

Molecular biology

To obtain a pcDNA3-FLAG fusion vector, the FLAG (DYKDDDDK) epitope was introduced in the *Xba*I and *Apa*I sites of pcDNA3 (Clontech). For C-terminal fusion of rat TRPV1 and murine TRPV2 to TRPV6 with the FLAG epitope or the cyan (CFP) and yellow (YFP) variants of the green fluorescent protein, stop codons were replaced by in-frame *Xba*I (TRPV1, -3 and -4) or *Xho*I (TRPV2, -5 and -6) restriction sites by PCR-mediated mutagenesis and subsequent subcloning into pcDNA3-CFP, pcDNA3-YFP (Schaefer et al., 2001) or pcDNA3-FLAG fusion vectors. Deletion mutants of TRPV1 were generated by PCR. For constructing chimeras of TRPV1 and TRPV4 or TRPV3, the cDNA corresponding to transmembrane domains and/or cytosolic termini were constructed by PCR, flanked by *Bsm*BI restriction sites and subsequently combined by in-frame ligation. To ensure a minimally disturbed secondary or tertiary structure of chimeras, highly conserved amino acids were selected for transition between the cytosolic termini and transmembrane domains. N-terminal exchanges were located in a (D/T)KWX(R/K)F motif preceding the first transmembrane domain (site of cDNA ligation underlined). C-terminal exchanges were generated in the LIALMGE motif at the end of the sixth transmembrane segment. All constructs were confirmed by cDNA-sequencing on an ABI-Prism 377 sequencer (Perkin Elmer, Norwalk, CT).

Cell culture and transient transfection

Human embryonic kidney (HEK) 293 cells (ATCC, Manassas, VA) were maintained at 37°C under 5% CO_2 in minimal essential medium with Earle's salts supplemented with 10% foetal bovine serum, 100 μg/ml streptomycin and 100 U/ml penicillin. Cells were transiently transfected using Fugene 6 transfection reagent (Roche Molecular Biochemicals, Mannheim, Germany) following the manufacturer's instructions. For fluorescence microscopy experiments, cells were seeded on glass coverslips. For confocal imaging of the subcellular localization of singular or coexpressed TRPV channels, cells were transfected with 2 μg of total plasmid cDNA per well. For FRET analysis, cells were transfected with 0.1-0.5 μg of plasmid cDNA encoding the CFP-tagged TRPV channel subunit and 1.5-1.9 μg of plasmid encoding the respective YFP-tagged subunit. In all FRET experiments, the molar ratio between CFP- and YFP-tagged TRPV channel subunits was adjusted to ~0.8-3.0, as detected by the comparing fluorescence intensities of coexpressed TRPV subunits to that of an intramolecularly linked CFP-YFP tandem protein as described previously (Lenz et al., 2002).

For coimmunoprecipitation experiments, cells were transfected in 60 mm dishes with a total amount of 4 μg of plasmid cDNA encoding FLAG- (1.5-2 μg/well) and YFP-tagged (2-2.5 μg/well) TRPV channels. All experiments were performed 1 day after transfection.

Confocal imaging procedures

A confocal laser-scanning microscope (LSM 510-META, Carl Zeiss, Jena, Germany) and a Plan-Apochromat 63×/1.4 NA objective were used for confocal imaging experiments. CFP- or YFP-tagged TRPV channels were alternately excited with the 458 nm or 488 nm laser lines of an argon laser. Emission filters were a 460-500 nm band pass for CFP and a 505 nm long pass for YFP. Pinholes were adjusted to yield optical sections of 0.6-0.9 μm. Correlation coefficients r^2 describing the colocalization of differently tagged TRPV subunits were determined using Pearson correlation analysis after displaying the scatter histogram of CFP and YFP pixel intensities (Zeiss, LSM510 software 3.2). Additional information is provided in supplementary material Fig. S1.

Fluorescence resonance energy transfer (FRET) determination and digital video imaging

FRET and imaging of the cytosolic Ca^{2+} concentration ($[Ca^{2+}]_i$) were carried out in a monochromator-equipped digital video imaging system (TILL-Photonics, Gräfelfing, Germany) attached to an inverted epifluorescence microscope (Axiovert 100, Carl Zeiss). All imaging experiments were performed in a HEPES-buffered solution containing 138 mM NaCl, 6 mM KCl, 1 mM $MgCl_2$, 1 mM $CaCl_2$, 5.5 mM glucose, 2 mg/ml BSA and 10 mM HEPES, pH 7.4. Loading of fura-2/AM (2 μM) and subsequent single-cell determination of the $[Ca^{2+}]_i$ or of the total fura-2 fluorescence were done as described previously (Schaefer et al., 2000). Bleeding of CFP and YFP signals into the fura-2 channels was eliminated by a spectral multivariate linear regression analysis (Lenz et al., 2002).

FRET efficiencies were determined by monitoring the increase in the CFP (FRET-donor) fluorescence emission during selective YFP (FRET-acceptor) photobleaching. The photobleaching protocol consisted of 15 cycles with 40 mseconds/cycle exposures at 410 nm for CFP detection and 8 mseconds per cycle at 515 nm for YFP detection. During the following 60 cycles, YFP was photobleached by applying an additional 2.1 seconds/cycle illumination at 512 nm, yielding about 12% bleach per cycle (objective: Plan-Apochromat 63×/1.4 NA, Carl Zeiss). For each FRET experiment the relative CFP and YFP fluorescence intensities ($[CFP]_r$ and $[YFP]_r$) of single cells were determined and normalized based on an intramolecularly fused CFP-YFP tandem protein (Hellwig et al., 2004). Therefore, we could assess the molar ratio between the FRET donor (CFP-tagged subunit) and FRET acceptor (YFP-tagged subunit), and only cells in which the acceptor-to-donor ratio exceeded 0.8 (giving rise to more than 83% of the maximal FRET efficiency) (Amiri et al., 2003) were included in the calculation of FRET efficiencies. In each experiment, data of 4-8 single cells with appropriate molar ratio were averaged. Means and s.e. were computed from three to ten independent bleach experiments for each combination of CFP- and YFP-fused TRPV subunits.

Coimmunoprecipitation and immunoblot analysis

HEK293 cells were transiently transfected and grown to about 80% confluence in a 60 mm dish and harvested in PBS. After centrifugation for 10 minutes at 100 ***g***, cells were aspirated through a 26-gauge needle in 2 ml ice-cold buffer containing 1 mM EDTA, 10 μg/ml aprotinin, 10 μg/ml leupeptin and 50 mM HEPES, pH 7.5. Membranes were pelleted (15 minutes at 12,000 ***g***, 4°C), and pellets were solubilized in 600 μl ice-cold lysis buffer containing 150 mM NaCl, 1 mM EDTA, 1% NP-40, 0.5% deoxycholate, 0.1% SDS, 10 μg/ml aprotinin, 10 μg/ml leupeptin and 20 mM Tris-HCl, pH 7.5. Particulate material was removed by centrifugation for 20 minutes at

12,000 ***g***, 4°C. TRPV proteins were immunoprecipitated by incubating 500 µl supernatant with 4 µg anti-FLAG M2 monoclonal antibody (Sigma, Deisenhofen, Germany) for 5 hours at 4°C, followed by overnight incubation at 4°C with 11 µg/ml protein A-Sepharose (Sigma). Immunoprecipitates were washed three times with 1 ml lysis buffer. Membrane lysates and immunoprecipitates were subjected to SDS gel electrophoresis (8% polyacrylamide) and blotted on nitrocellulose. After blocking for 1 hour at 22°C with 5% non-fat dry milk in TBS, blots were probed either with an anti-FLAG M2 monoclonal antibody (Sigma; 1:1000) or with a polyclonal rabbit anti-GFP antibody (Clontech; 1:1000) in blocking buffer at 4°C overnight. Secondary antibodies were peroxidase-conjugated anti-rabbit IgG (1:2000) or anti-mouse IgG (1:5000) antibodies (Sigma). Peroxidase activity was detected with a chemiluminescence detection reagent (AppliChem, Darmstadt, Germany).

Results

To investigate the formation of heteromeric channel complexes within the TRPV subfamily, we characterized fluorescent fusion proteins of TRPV1-6 channel subunits in living cells as well as their interaction with FLAG-tagged TRPV subunits. To validate the constructs, we tested the channel function and the cellular localization in HEK293 cells. The regulatory and biophysical properties of TRPV1-YFP were indistinguishable from those of wild-type TRPV1 in terms of cation selectivity, I/V-relationship, activation by capsaicin, endovanilloids, heat or extracellular protons as detected by patch-clamp and Ca^{2+} imaging experiments (data not shown). In Ca^{2+} imaging and Mn^{2+} quench experiments, TRPV2-YFP and TRPV3-YFP were activated at temperatures higher than 52°C and 37°C, respectively, and TRPV4-YFP responded to both 4α-phorbol 12,13-didecanoate and hypotonic extracellular solutions. In whole cell patch-clamp experiments, TRPV5-YFP and TRPV6-YFP conferred a constitutive Ca^{2+} entry pathway exhibiting current-voltage relationships indistinguishable from those of cells expressing the respective wild-type channels. Like wild-type TRPV5 and TRPV6, TRPV5-YFP and TRPV6-YFP could be blocked by La^{3+} or ruthenium red.

Expression and subcellular localization of TRPV channels in HEK293 cells

To assess the compartmentalization of TRPV channels in living cells, expression plasmids encoding YFP-fused TRPV channels were transiently transfected in HEK293 cells, and fluorescent fusion proteins were imaged by confocal laser-scanning microscopy. TRPV1-YFP was mostly present in intracellular compartments such as the endoplasmic reticulum and a smaller fraction was located in the plasma membrane (Fig. 1A). The retention of TRPV1 and other TRPV channel subunits in the endoplasmic reticulum was verified by co-transfection of a CFP construct fused to a KDEL endoplasmic reticulum targeting motif (pECFP-Endo, Clontech, data not shown). By contrast, TRPV2-YFP and TRPV3-YFP were efficiently targeted to the plasma membrane and displayed a homogenous distribution along the plasma membrane (Fig. 1B,C). Minor fractions of TRPV2-YFP and TRPV3-YFP were retained in the endoplasmic reticulum, depending on the expression level and the time after transfection. If analyzed in more detail, an accumulation of TRPV2-YFP was observed in small and dynamically forming and retracting protrusions of the plasma membrane presumably representing filopodia (data not shown). For TRPV4-YFP, we observed a clustered distribution in structures that overlap with the endoplasmic reticulum and the plasma membrane (Fig. 1D). TRPV5-YFP and TRPV6-YFP were mostly observed in intracellular vesicular compartments (Fig. 1E,F). Even at the highest possible resolution, we were unable to detect a fluorescence enhancement over the plasma membrane. As TRPV4-YFP, TRPV5-YFP and TRPV6-YFP, like their wild-type counterparts (Strotmann et al., 2000; Hoenderop et al., 1999; Vennekens et al., 2000; Peng et al., 1999), form constitutively active and Ca^{2+}-permeable cation channels (data not shown), cell survival possibly requires retention in endomembranes or an efficient internalization from the plasma membrane to endosomal structures.

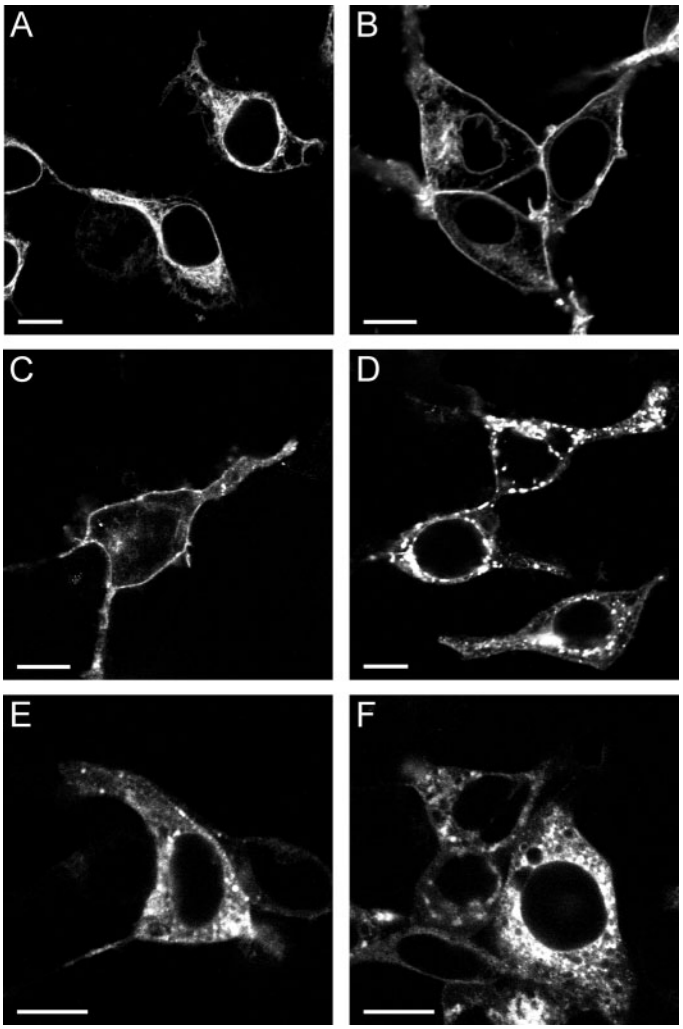

Fig. 1. Expression and subcellular localization of TRPV channels. Rat TRPV1 (A) and murine TRPV2 to TRPV6 (B-F) were C-terminally fused to YFP, and plasmids were transiently transfected in HEK293 cells. Cells were imaged by confocal laser-scanning microscopy 1 day after transfection. The pinholes were adjusted to obtain optical sections with a thickness of ~0.6 µm. Typical expression patterns of the different TRPV channels from three to five independent transfections are shown. Bar, 10 µm.

Subcellular localization of coexpressed TRPV channel subunits

Because heterologously expressed TRPV channel subunits exhibited a differential subcellular localization pattern, a first indication of heteromeric TRPV channel assembly may be obtained by assessing the subcellular localization of coexpressed CFP- or YFP-fused TRPV channel subunits in HEK293 cells. Colocalization or redistribution upon coexpression of different channel subunits may indicate an assembly into heteromeric channel complexes whereas a distinct localization pattern alludes to an independent and homo-oligomeric assembly of coexpressed TRPV channel subunits. A statistical pixel-based analysis was applied to assess correlation coefficients of CFP and YFP pixel intensities. These correlation coefficients (r^2) can be roughly grouped into r^2=0.4-1.0 for very good colocalization, 0.1-0.4 for partial colocalization and 0-0.1 for mostly distinct localization. When TRPV1-YFP was coexpressed with TRPV2-CFP at molar ratios of 1:1 to 1:3, confocal laser-scanning microscopy revealed a partial overlap of the fluorescence in intracellular compartments and in the plasma membrane with a correlation coefficient of the fluorescence intensities of 0.30 (Fig. 2A). By contrast, upon coexpression of TRPV1-YFP and TRPV3-CFP or of TRPV1-YFP and TRPV4-CFP, the TRPV subunits maintained their differential subcellular localization, resulting in poor colocalization and low correlation coefficients of 0.18 and 0.13, respectively (Fig. 2B,C compared to Fig. 1A,C,D). Coexpression of TRPV2 and TRPV3 resulted in almost identical fluorescence patterns (Fig. 2D), an effect that could be expected as both channels were efficiently targeted to the plasma membrane if expressed alone (see Fig. 1B,C). HEK293 cells coexpressing TRPV2/TRPV4 or TRPV3/TRPV4 displayed almost no overlapping localization of the respective channel subunits (Fig. 2E,F), thus precluding an efficient heteromeric assembly of these TRPV subunits. Likewise, the cellular localization of TRPV2 or TRPV3 displayed no significant overlap with that of TRPV5 or TRPV6 expressed in the same cells (r^2<0.1; Fig. 2G,H and Table 1). When TRPV5 was coexpressed with its phylogenetically closest relative, TRPV6, identical localization was discernible in vesicular intracellular structures (Fig. 2I). Data of all possible permutations of combinatorial coexpression of different TRPV channel subunits are summarized in Table 1. The observed different localization patterns of most combinations of coexpressed TRPV channel subunits point to a restricted promiscuity of heteromeric TRPV channel assembly.

Fluorescence resonance energy transfer between TRPV channel subunits

To explore the assembly of different TRPV channel subunits, we assessed the proximity of coexpressed CFP- and YFP-tagged TRPV channel subunits in HEK293 cells by fluorescence resonance energy transfer (FRET). FRET efficiencies were determined by measuring the donor recovery

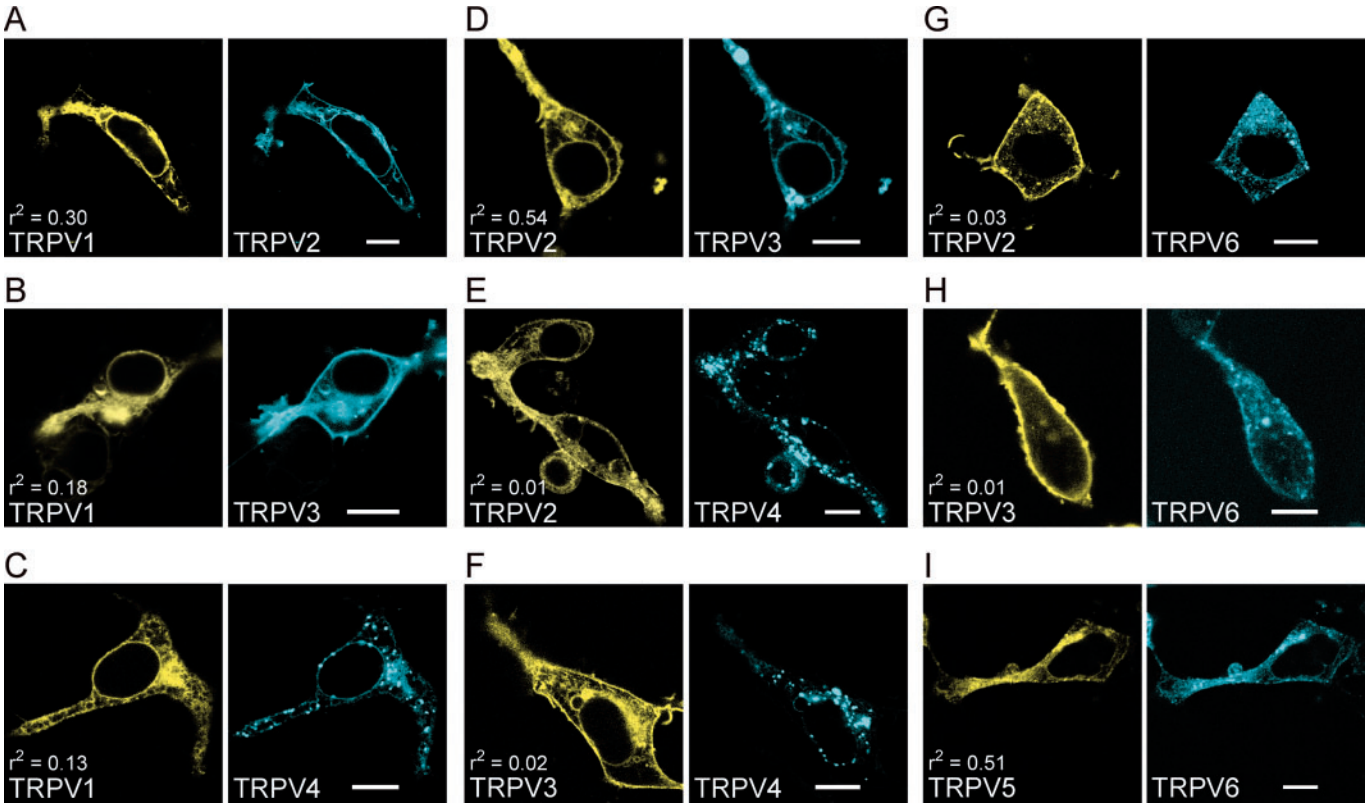

Fig. 2. Subcellular localization of coexpressed TRPV channel subunits. (A-I) Different combinations of TRPV channels tagged with either CFP or YFP were coexpressed in HEK293 cells and sequentially imaged by confocal laser-scanning microscopy in the same cell. For each coexpression experiment, the correlation coefficient between CFP and YFP fluorescence intensities (r^2) was estimated by pixel-based image analysis. Shown are representative data of three independent transfections. Bars, 10 μm.

Table 1. Quantitative colocalization analysis of coexpressed TRPV channel subunits

	TRPV1	TRPV2	TRPV3	TRPV4	TRPV5
TRPV2	0.31±0.03				
TRPV3	0.13±0.03	0.45±0.02			
TRPV4	0.12±0.01	0.04±0.01	0.05±0.01		
TRPV5	0.03±0.01	0.03±0.01	0.06±0.01	0.04±0.01	
TRPV6	0.05±0.02	0.04±0.01	0.04±0.01	0.06±0.02	0.52±0.02

Various YFP- and CFP-tagged TRPV subunits were coexpressed in HEK293 cells, and expression patterns were imaged by confocal laser-scanning microscopy. CFP and YFP pixel intensities of differently tagged TRPV subunits were subjected to Pearson correlation analysis to obtain correlation coefficients r^2 describing the colocalization. Shown are mean±s.e. of five to fifteen cells from two to four independent transfection experiments.

during selective photobleaching of the acceptor. To ensure appropriate conditions for FRET formation, the relative CFP and YFP fluorescent intensities were determined and the molar ratio between coexpressed fluorescent donor and acceptor TRPV channel subunits was adjusted to >0.8 (YFP:CFP) in all FRET experiments (Amiri et al., 2003). Each TRPV channel, in its homo-oligomeric state, displayed a FRET efficiency of at least 9.5%, thus confirming that each fluorescent TRPV fusion protein is capable of forming homomultimers (Fig. 3A). Upon coexpression of different TRPV subunits, the FRET-efficiency between TRPV1 and TRPV2 was higher compared to those between TRPV1 and other TRPV subunits (Fig. 3B). Of note, the FRET efficiency (8.4±0.4%) was lower than the values of the respective homomultimers (15.8±0.4% for TRPV1 and 12.0±0.5% for TRPV2). When TRPV1 was coexpressed with TRPV3, -4, -5 or -6, FRET efficiencies were between 2.3% and 3.8%. In combinatorial coexpression experiments with TRPV4-YFP as the FRET acceptor, a high FRET efficiency of 25±1.5% could be demonstrated exclusively for the homomultimeric conformation, but not with any other TRPV channel subunit (Fig. 3C). Coexpressed TRPV5 and TRPV6 gave rise to a FRET efficiency of 18.3±0.4%, which is even higher than the values of the respective homomultimers (Fig. 3D). If any other of the possible TRPV channel subunits were coexpressed, some combinatorial TRPV expressions failed to exhibit FRET, indicating a lack of heteromer formation, whereas others had low FRET efficiencies of 2.0-4.4% which were less than half of the FRET efficiencies between the respective homomultimers (data not shown). Thus, FRET data point to an efficient heteromultimerization occurring only between TRPV5 and TRPV6. An interaction between TRPV1 and TRPV2 subunits appears likely, but may occur with a lower efficiency compared to the formation of the respective homo-oligomers.

Coimmunoprecipitation of TRPV channel subunits

To assess the heteromeric assembly of TRPV channels by an independent biochemical approach, coimmunoprecipitation experiments were performed. TRPV channels were fused to a FLAG epitope tag at their C termini and coexpressed together with YFP-tagged TRPV channels at various combinations in HEK293 cells. After membrane preparation and solubilization, FLAG-tagged TRPV channels in the lysates were immunoprecipitated with anti-FLAG antibodies. Membrane lysates and immunoprecipitates were subjected to SDS-gel electrophoresis and probed with anti-GFP or anti-FLAG antibodies to visualize co-purified TRPV channel subunits and the recovery of the respective immunoprecipitated TRPV-FLAG channels, respectively (Fig. 4). For all homomultimeric combinations, coimmunoprecipitation was clearly discernible (see Fig. 4A-E, middle panels). Coexpression of TRPV1-FLAG and TRPV2-YFP resulted in lower coimmunoprecipitation efficiencies as compared to the TRPV1-FLAG/TRPV1-YFP homomer (Fig. 4A). The coimmunoprecipitation of TRPV1 and TRPV2 could be verified in the reciprocal experiment (TRPV2-FLAG/TRPV1-YFP; Fig. 4B). Coimmunoprecipitation between TRPV1-FLAG and TRPV3-YFP or TRPV4-YFP or of TRPV2-FLAG

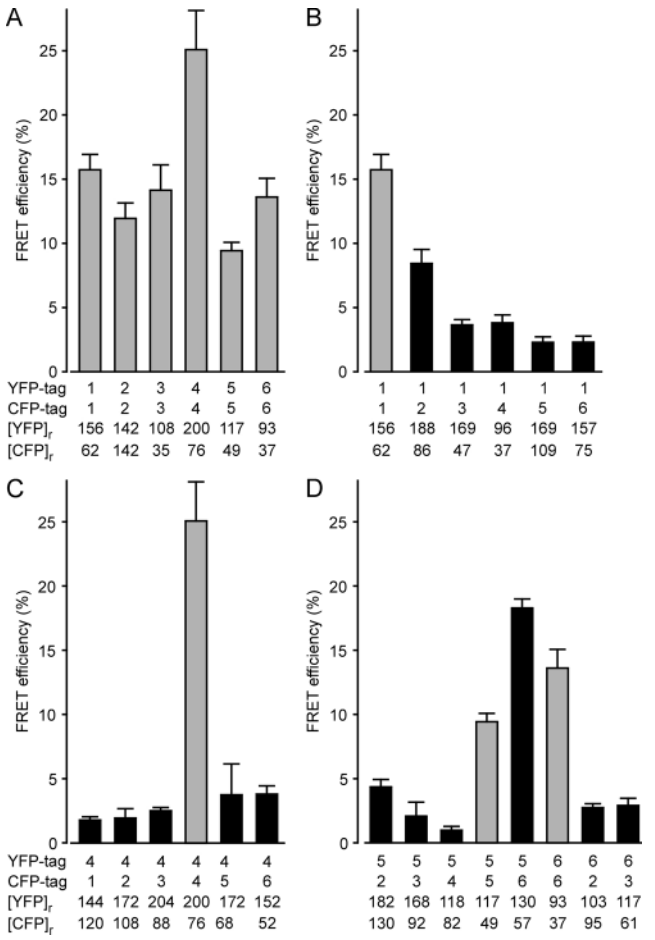

Fig. 3. Determination of FRET between TRPV channel subunits. (A-D) HEK293 cells were transiently co-transfected with expression plasmids encoding CFP- or YFP-fused TRPV channels as indicated. The relative CFP and YFP fluorescence intensities in single cells expressing the respective TRPV construct were determined and averaged ($[CFP]_r$ and $[YFP]_r$) to ensure comparable TRPV expression. FRET efficiencies were determined by measuring the recovery of CFP fluorescence during YFP photobleaching. Cells were excited at 410 nm and 515 nm for CFP and YFP detection, respectively. YFP was bleached with an illumination at 512 nm for 2.1 seconds. FRET efficiencies between identical TRPV channel subunits are shown as grey bars. FRET experiments between different channel subunits are shown as black bars. Bars represent mean±s.e. of at least three independent experiments.

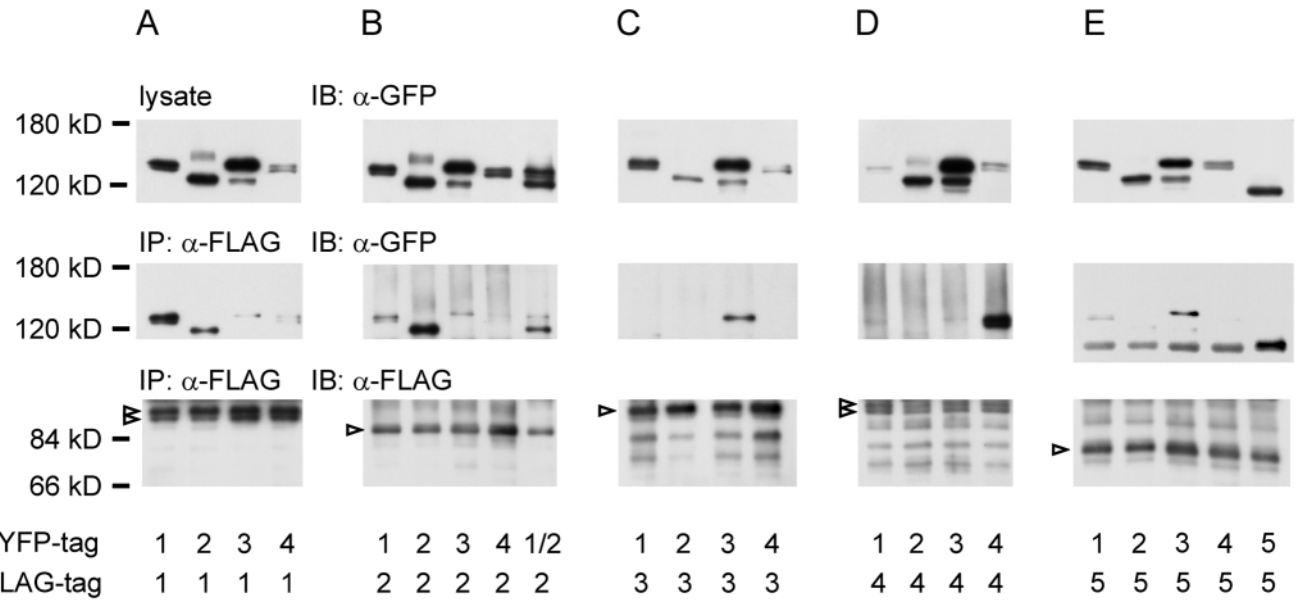

Fig. 4. Coimmunoprecipitation of TRPV channel subunits. (A-E) Plasmids encoding FLAG-tagged or YFP-tagged TRPV channels were co-transfected in HEK293 cells in the combinations indicated below the panels. One day after transfection, membranes were solubilized and lysates were immunoprecipitated (IP) with anti-FLAG antibodies. Membrane lysates (upper panels) or immunoprecipitates (middle and lower panels) were separated by SDS-PAGE. Upper and middle panels, TRPV in the membrane lysates and coprecipitated TRPV channels were detected by immunoblotting (IB) with anti-GFP antibodies. The recovery of the respective immunoprecipitated TRPV-FLAG channel is shown in the lower panels by probing blots with anti-FLAG antibodies. Arrowheads indicate the expected sizes of the respective TRPV-FLAG channel subunits.

and TRPV3-YFP or TRPV4-YFP was either poor (Fig. 4A,B) or not reproducible in the reciprocal experiment (Fig. 4C,D). To test whether homo- and hetero-oligomeric assembly of TRPV1 and TRPV2 occurred with comparable affinities, we took advantage of the different gel mobility of TRPV1 and TRPV2 and performed a coimmunoprecipitation experiment with HEK293 cells coexpressing TRPV2-FLAG together with equal amounts of TRPV1-YFP and TRPV2-YFP (Fig. 4B, upper panel right lane). Both YFP-tagged channel subunits were co-purified in the immunoprecipitates, but the TRPV2 homomultimer was clearly preferred over the hetero-oligomeric interaction of TRPV2-FLAG with TRPV1-YFP (Fig. 4B, middle panel). As experiments shown in each of the panels of Fig. 4 were performed in parallel and analyzed on the same gels, results of various combinatorial coexpressions can be compared to those of the respective homo-oligomer. The coimmunoprecipitation experiments shown here and data presented elsewhere (Hoenderop et al., 2003) on TRPV5 and TRPV6 corroborate the FRET and colocalization analyses demonstrating that, besides TRPV homo-oligomers, only TRPV1/TRPV2 or TRPV5/TRPV6, can coassemble into heteromeric complexes.

Cytosolic termini are required for TRPV1 assembly and function

In analogy to reports describing multimerization of other hexahelical cation channels as a function of the cytosolic N- or C-termini, we truncated TRPV1-YFP at various N- or C-terminal positions. Truncation of the N-terminus by 73 amino acids did not affect the TRPV1 localization or function. Omitting the first 118 or 179 amino acids of the TRPV1 peptide chain still yielded functional channels, but capsaicin-induced increases in $[Ca^{2+}]_i$ were weaker as compared to the full-length clone despite similar expression levels (Fig. 5A). Likewise, FRET efficiencies between the respective YFP-tagged truncated TRPV1 constructs and full-length TRPV1-CFP gradually decreased. Deletion of 233 and 295 N-terminal amino acids including the first and the second ankyrin-like repeat, respectively, resulted in a loss of capsaicin-induced channel activity. Moreover, upon C-terminal fusion to YFP, $TRPV1_{\Delta 1\text{-}233}$ exhibited only weak FRET signals if coexpressed with TRPV1-CFP, indicating loss of assembly with full-length TRPV1.

A step-wise deletion of C-terminal moieties of TRPV1 had a similar effect. Truncation of up to 73 amino acids did not significantly impede on the capsaicin-induced channel activation, whereas capsaicin-induced increases in $[Ca^{2+}]_i$ were gradually or completely abrogated upon deletion of 93 and 110 C-terminal amino acids, respectively (Fig. 5B). The fluorescence of YFP fused to the functionally defective mutant $TRPV1_{\Delta 729\text{-}838}$ was mislocalized to intracellular vesicles, and fluorescence was detectable even in the cytosol, possibly as a consequence of limited proteolysis. In addition, overexpression of $TRPV1_{\Delta 729\text{-}838}$ (not fused to a fluorescent protein) together with CFP- and YFP-fused full-length TRPV1 failed to compete for the assembly of the full-length channel subunits as detected by competitive-FRET analysis. As a possible ATP/GTP-binding site motif (Walker A-type) is located in amino acids 729-735 of TRPV1, we excised this putative structural motif in $TRPV1_{\Delta 729\text{-}735}$ and found no channel function. However, as the replacement of amino acids 729-735 in TRPV1 by alanine residues did not disrupt the channel function, we conclude that the Walker A motif itself

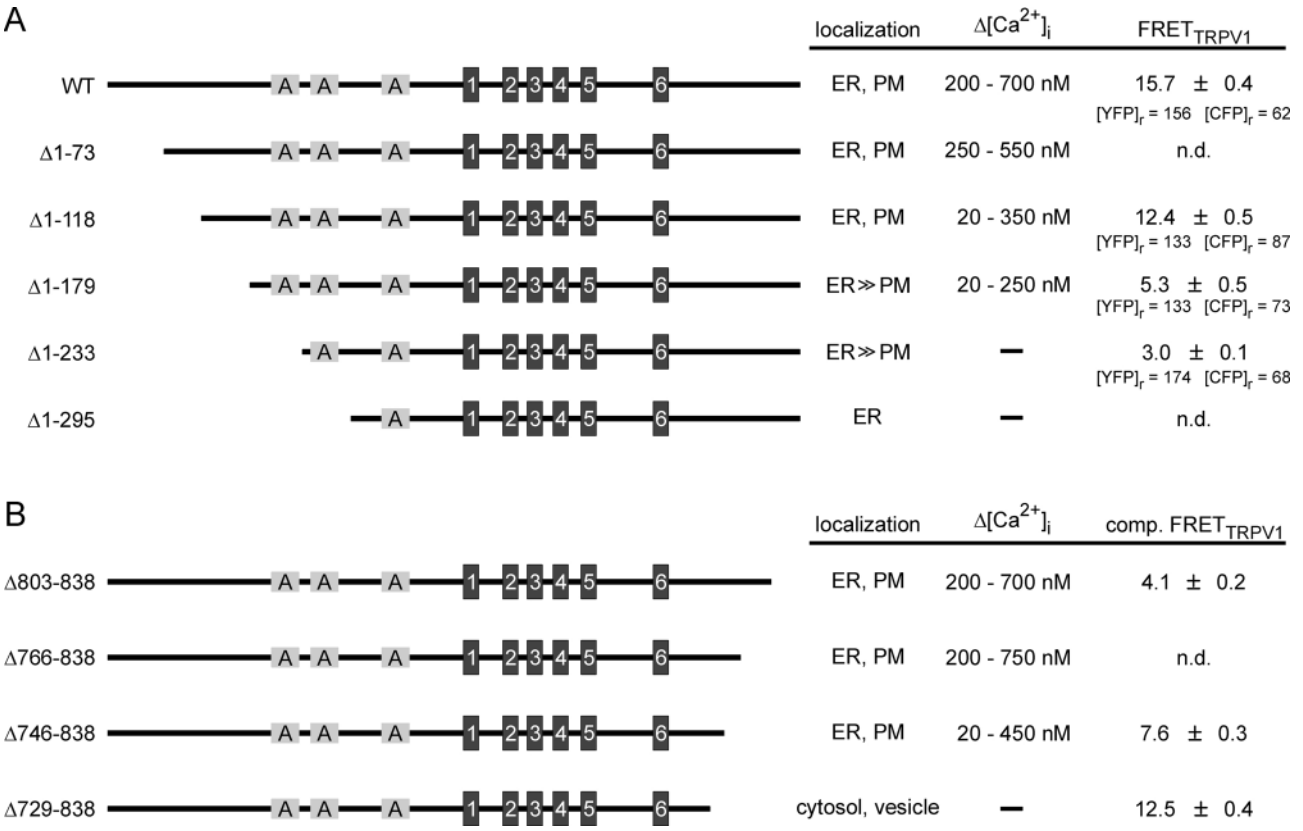

Fig. 5. Cytosolic termini are required for TRPV1 assembly and function. Schematic representation of N-terminal (A) and C-terminal (B) TRPV1 deletion mutants showing the ankyrin repeats (indicated as A) and the six transmembrane domains (1-6). WT represents full-length rat TRPV1. The numbers on the left indicate deleted amino acids. The table summarizes the data on the intracellular location of C-terminally YFP-tagged deletion mutants imaged by confocal laser-scanning microscopy, of the capsaicin-induced maximal increases in the intracellular Ca^{2+} concentrations ($\Delta[Ca^{2+}]_i$), and of FRET efficiencies between mutants and full-length TRPV1 (A) or of FRET efficiencies in competition experiments with CFP- and YFP-tagged TRPV1 and non-tagged deletion mutants (B). $[YFP]_r$ and $[CFP]_r$ represent averaged relative fluorescence intensities of YFP-tagged TRPV1 or the N-terminal TRPV1 deletion mutants and TRPV1-CFP. Data are the mean±s.e. of four to eleven independent FRET experiments. ER, endoplasmic reticulum; PM, plasma membrane.

is not necessary for the interaction. We conclude that, although both termini are required for TRPV1 channel function and assembly, the assignment of interacting domains is complicated by secondary effects possibly involving protein folding, stability or targeting.

Assembly of chimeric TRPV channel subunits

To study the relative contribution of N- or C-termini as well as of the transmembrane domain to the overall affinity between TRPV channel subunits, we constructed a set of chimeric TRPV channel subunits composed of parts of the phylogenetically related, but poorly interacting TRPV1 and TRPV4 channels. A simplified nomenclature of these constructs is outlined in Fig. 6A. According to this nomenclature, a $TRPV_{4.1.4}$ construct contains the cytosolic N- and C-termini of TRPV4 fused to the transmembrane segments of TRPV1. These constructs were again C-terminally fused to CFP or YFP and subjected to quantitative FRET analysis in living HEK293 cells by recording the donor unquenching during selective photobleaching of the acceptor.

To our surprise, most constructs exhibited high FRET efficiencies (>10%) upon combinatorial coexpression with TRPV1 or with other chimeras (Fig. 6B,D). Assuming that the cytosolic N-termini control the TRPV channel assembly, we would expect that interaction between $TRPV_{4.1.1}$ and TRPV1 is weak. Our data, however, demonstrate that N- or C-termini of TRPV1 can be freely replaced by those of TRPV4 without losing the ability to form oligomers with TRPV1 exhibiting FRET efficiencies of about 15-20% (Fig. 6B,D). We conclude that the transmembrane domain of TRPV1 contributes significantly to the channel assembly. In agreement with this model, coexpressed $TRPV_{1.4.1}$ and $TRPV_{4.1.4}$, sharing neither N- or C-termini nor a common transmembrane domain, displayed no significant FRET efficiency (Fig. 6D). $TRPV_{4.1.4}$ and $TRPV_{4.1.1}$ efficiently interacted with both TRPV1 and TRPV4 (Fig. 6B,C). This promiscuity points to a major contribution of the cytosolic N-terminus, rather than of the transmembrane domain or C-terminus, to the assembly of TRPV4 subunits. In contrast to TRPV4, cytosolic C- and N-termini of TRPV1 were not sufficient to overcome non-compatible transmembrane domains as evidenced by a low FRET efficiency (3%) between $TRPV_{1.4.1}$ and TRPV1 compared to the FRET signal of 15.8% between TRPV1 homomultimers (see Fig. 6B). Hence, depending on the TRPV isoform, a dominant contribution to the interaction appears to

be conferred either by the transmembrane domain (TRPV1) or by the cytosolic termini (TRPV4).

Interaction between cytosolic TRPV1 and TRPV4 termini

To test the hypothesis that cytosolic termini differentially contribute to TRPV channel assembly, we coexpressed CFP- or YFP-fused cytosolic termini of TRPV1 or TRPV4 and tested for an interaction between them by FRET analysis in living cells. Fluorescent tags were fused to the respective native ends of the cytosolic N- or C-termini of TRPV1 or TRPV4 and were detectable as soluble protein in the cytosol and, in some cases, also in the nucleus of living HEK293 cells. For soluble CFP- and YFP-fused termini of TRPV1, FRET efficiencies of 1.9±0.6% (N-termini), 3.5±0.9% (C-termini), and 1.1±0.5% (between N- and C-termini) were obtained (Fig. 7A). If coexpressed with C-terminally or N-terminally tagged full-length TRPV1, the

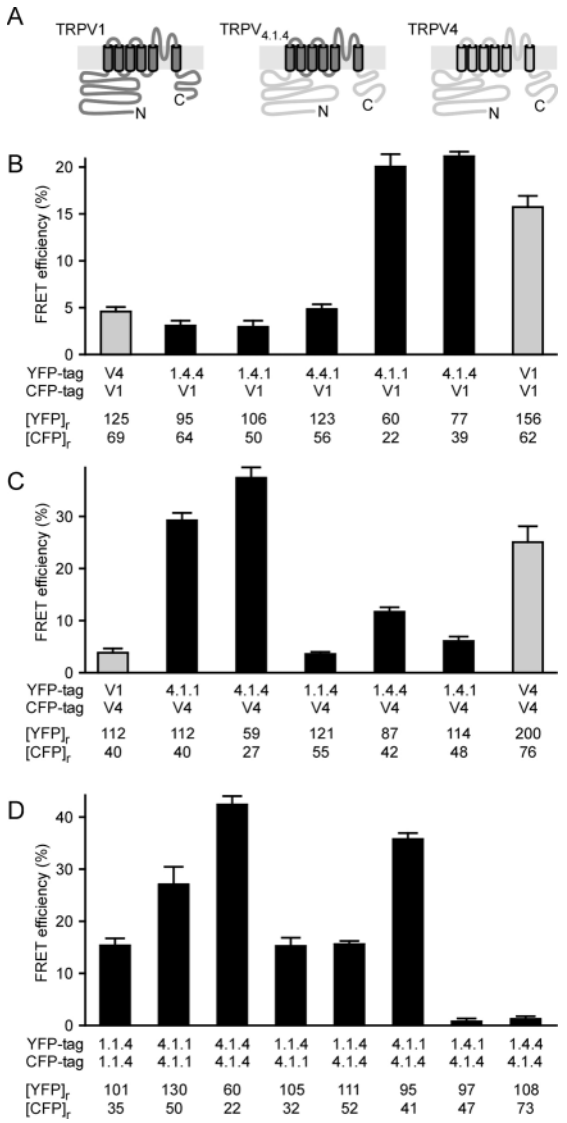

Fig. 6. Assembly of chimeric TRPV channel subunits. (A) Chimeric TRPV channel subunits were constructed consisting of various combinations of the cytosolic N- or C-termini and the transmembrane domains of TRPV1 and TRPV4. (B-D) HEK293 cells were transiently co-transfected with expression plasmids encoding CFP- or YFP-fused TRPV channels or TRPV channel chimeras as indicated. FRET efficiencies (means±s.e.) were determined as described in Fig. 3. Grey bars, FRET efficiencies of only full-length TRPV channel subunits; black bars, FRET experiments with TRPV channel chimeras. $[YFP]_r$ and $[CFP]_r$ represent means of the CFP and YFP fluorescence intensities.

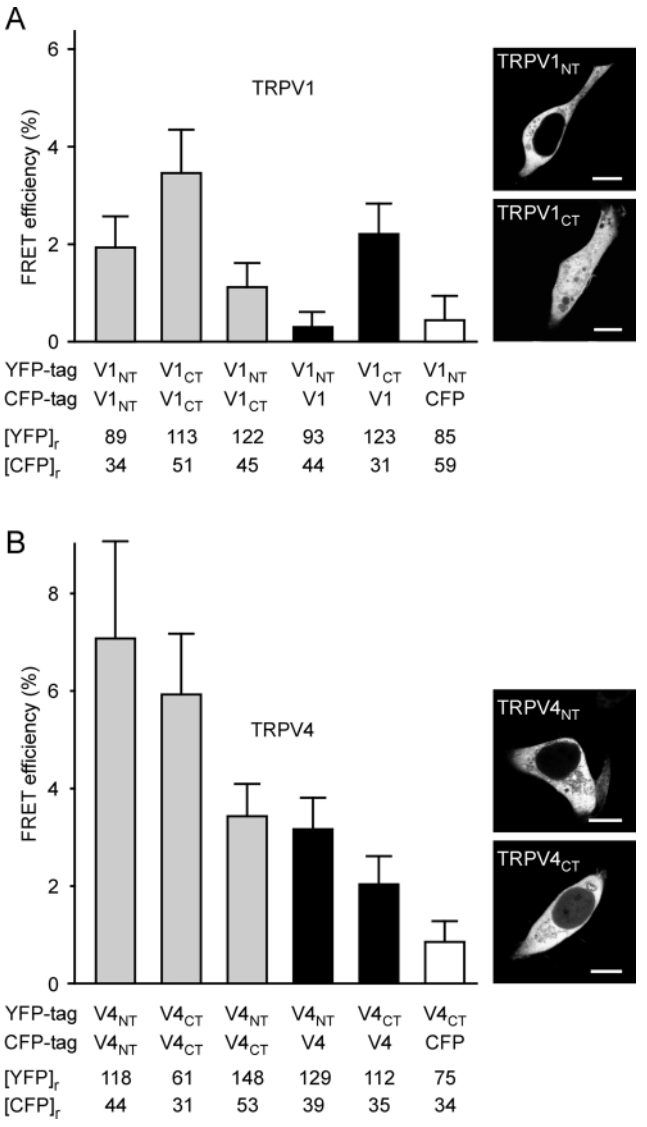

Fig. 7. Interaction between cytosolic TRPV1 and TRPV4 termini. (A,B) Cytosolic N- and C-termini (NT, CT) of TRPV1 (A) or TRPV4 (B) tagged with either CFP or YFP were coexpressed in HEK293 cells as indicated and subjected to quantitative FRET analysis. Bars in panels A and B represent FRET efficiencies (means±s.e.) among TRPV termini (grey bars), TRPV termini and full-length TRPV channels (black bars) and, as a control, between TRPV termini and soluble CFP (white bars). Data shown are representative of at least three independent experiments. The average relative fluorescence intensities ($[YFP]_r$ and $[CFP]_r$) indicate the relative expression levels of the respective TRPV constructs. (Insets) Confocal images showing typical localization of the YFP-tagged TRPV termini in HEK293 cells (bars, 10 μm).

soluble TRPV1 N-terminus was not recruited to the membrane compartment and displayed FRET efficiencies below 1% (data not shown).

Upon coexpression of differentially tagged soluble termini of TRPV4 (Fig. 7B), we observed FRET efficiencies of 7.1±2% (N-termini), 5.9±1.3% (C-termini) or 3.4±0.7% (between N- and C-termini). One should note that N-terminally CFP- and YFP-fused full-length TRPV4 yields FRET efficiencies of 12% (data not shown) whereas C-terminally tagged full-length TRPV4 exhibited FRET signals about 25% (see Fig. 3A). Thus, although FRET efficiencies between full-length TRPV1 or TRPV4 subunits are in general higher than those between their soluble termini, only the cytosolic N-terminus of TRPV4 with itself or full-length TRPV4 exhibited FRET efficiencies similar to those seen in the N-terminally tagged full-length TRPV4 (Fig. 7B).

However, both cytosolic termini of TRPV1 or TRPV4 showed no dominant-negative effect regarding channel activity in Mn^{2+}-quench experiments when coexpressed in a 5- to 15-fold molar excess with the respective full-length TRPV channels (data not shown). Thus, these data support the hypothesis that TRPV1 assembly is mainly conferred by determinants located in the transmembrane domain and to some extent maybe supported by its cytosolic C-terminus. For TRPV4 subunit assembly, important interaction determinants are located in the cytosolic N-terminus and additional stabilization may require cooperative interaction sites located in the C-terminus and in the transmembrane domain.

N-termini of non-interacting TRPV subunits can functionally substitute for the native N-terminus of TRPV1 or TRPV4

As outlined above, truncation of the TRPV1 N-terminus by 233 or 295 amino acids resulted in a loss of capsaicin-induced channel activation and assembly with full-length TRPV1 (Fig. 5A). As the chimeric $TRPV_{4.1.1}$ construct in its homo-oligomeric state exhibited FRET efficiencies of 27% (see Fig. 6D), we wondered whether fusion to N-termini of non-interacting TRPV subunits may also rescue channel function. Indeed, $TRPV_{4.1.1}$-expressing, fura-2-loaded HEK293 cells responded to the addition of 10 μM capsaicin with an immediate increase in $[Ca^{2+}]_i$ (data not shown) and, in the presence of 250 μM Mn^{2+}, displayed a robust acceleration of Mn^{2+} entry (Fig. 8A). The quench rate of the fura-2 fluorescence during a 30-second interval was 0.14% per second before and 1.5% per second after the addition of capsaicin. In addition, we constructed a chimera containing the cytosolic N-terminus of TRPV3 fused to the transmembrane domain and the C-terminus of TRPV1 ($TRPV_{3.1.1}$). These $TRPV_{3.1.1}$ subunits C-terminally tagged with YFP or CFP displayed FRET efficiencies of 8%, indicating that $TRPV_{3.1.1}$ chimeras are able to form homomultimers. Stimulation of $TRPV_{3.1.1}$-expressing cells with capsaicin again resulted in an about 20-fold increase in the Mn^{2+} entry upon capsaicin treatment (Fig. 8B). A $TRPV_{1.4.4}$ chimera again exhibited significant FRET efficiencies of 15% and responded to the addition of 4α-phorbol 12,13-didecanoate (5 μM) with a pronounced increase in Mn^{2+} permeability (Fura-2 fluorescence quenched by 0.015% per second before and 1.9% per second after stimulation; Fig. 8C). We conclude that the cytosolic N-termini of non-interacting TRPV channel isotypes can at least partially substitute for the respective native terminus to rescue oligomer formation and functional activity of the channel complex.

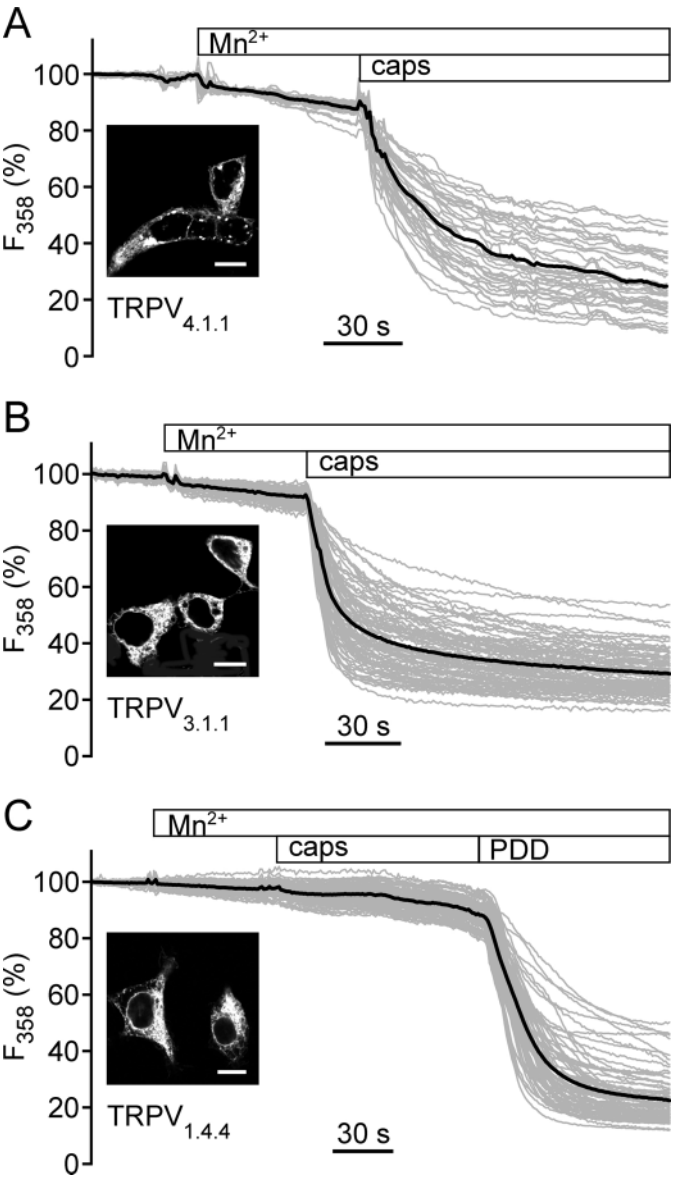

Fig. 8. Functional rescue of truncated TRPV1 or TRPV4 subunits by fusion with N-termini of related TRPV subunits. (A-C) Plasmids encoding YFP-tagged TRPV chimeras were transfected in HEK293 cells. In the presence of Mn^{2+} (250 μM), the cells were stimulated by adding 10 μM capsaicin (caps) or 5 μM 4α-phorbol 12,13-didecanoate (PDD) to the bath solution as indicated. Grey lines depict the time course of the total fura-2 fluorescence in single cells whereas the black lines represent the calculated means. The data are representative for three to four independent transfection experiments showing similar results. Insets show confocal micrographs of living HEK293 cells expressing the respective YFP-tagged TRPV chimera. Bar, 10 μm.

Discussion

As plasma membrane targeting of some of the YFP-tagged TRPV channels was poor, one may ask the question whether the fusion proteins behave differently compared to the corresponding wild-type proteins. With the exception of TRPV2-YFP and TRPV3-YFP, all other heterologously expressed TRPV channel subunits were mainly localized in intracellular compartments. Nonetheless, large cation currents were detectable in HEK293 cells expressing fluorescent fusion proteins of TRPV1, TRPV4, TRPV5 or TRPV6. Expression of TRPV1-YFP resulted in a staining of the endoplasmic reticulum and to a lesser degree the plasma membrane (Fig. 1A). A similar distribution has been shown for a TRPV1-GFP construct expressed in COS7 cells (Olah et al., 2001) as well as for native TRPV1 in small-to-medium diameter dorsal root ganglion neurons (Liu et al., 2003). Ca^{2+} mobilization from internal stores after application of resiniferatoxin or capsaicin on TRPV1-expressing cells and DRG neurons has been described consistently (Olah et al., 2001; Eun et al., 2001; Marshall et al., 2003). TRPV2-YFP and TRPV3-YFP were highly enriched in the plasma membrane. A preferential localization of TRPV2 in endomembrane compartments (Kanzaki et al., 1999) or even in the nucleus of NH15-CA2 neuroblastoma cells (Boels et al., 2001) was not evident in HEK293 cells. As TRPV2 is efficiently targeted to the plasma membrane in resting HEK293 cells, a secretion-coupling model put forward by the aforementioned studies may not operate in all cell models. For TRPV4-YFP, we observed a complex localization pattern. Most of the protein was enriched in clusters in endomembrane compartments, but an additional enhancement of the fluorescence at the nuclear membrane and at the plasma membrane was observed if cells were imaged with higher sensitivity. A predominantly intracellular localization of TRPV4 has been shown either for an epitope-tagged TRPV4 in HEK293 cells (Xu et al., 2003) or for native TRPV4 in keratinocytes (Chung et al., 2003). TRPV5-YFP or TRPV6-YFP were predominantly located in intracellular vesicular structures and, thus, confirm the localization pattern, which has been found for myc-tagged TRPV6 (Cui et al., 2002). Further experiments must clarify whether these intracellular structures result from internalization of TRPV5/6 protein or from a failure of nascent protein to pass the cellular quality control system. In addition, as native TRPV5 and TRPV6 channels are localized in the apical membrane of renal or intestinal epithelia (den Dekker et al., 2003), plasma membrane targeting of these channels may require additional proteins which are only present in polarized epithelial cells.

A co-targeting of intracellularly retained channel subunits by coexpression and heteromultimer formation with another TRP channel subunit has recently been evidenced for fluorescent fusion proteins of TRPC1 and TRPC4 (Hofmann et al., 2002). After coexpression of CFP- and YFP-tagged TRPV channels in HEK293 cells, co-trafficking of differently localized TRPV channels was not discernible indicating that a majority of possible permutations of coexpressed TRPV channels does not result in heteromeric channel assembly. A convincing colocalization was only observed for coexpressed TRPV1 and TRPV2, TRPV2 and TRPV3, or TRPV5 and TRPV6. As the overlap of fluorescence does not prove the existence of heteromeric TRPV channel complexes, we performed FRET experiments. Significant FRET efficiencies could be demonstrated for all homomultimeric TRPV channel combinations but only for two heteromultimeric combinations: TRPV1 and TRPV2, or TRPV5 and TRPV6. The interaction between TRPV1 and TRPV2 was confirmed by coimmunoprecipitation. However, western blot analyses showed that the formation of homomultimeric channel complexes is clearly preferred over the heteromeric assembly of TRPV1 and TRPV2. As the currently available expression studies indicate that TRPV1 and TRPV2 are mostly expressed in different tissues or cell types (Caterina et al., 1997; Tominaga et al., 1998; Caterina et al., 1999; Birder et al., 2002), the residual interaction between TRPV1 and TRPV2 may be without physiological relevance. Recently, the heteromultimerization of TRPV5 and TRPV6 has been studied and our results clearly confirm these data (Hoenderop et al., 2003). Furthermore, assembly of human TRPV1 and TRPV3 has been detected by coimmunoprecipitation experiments and functional assays (Smith et al., 2002). Neither colocalization analysis, nor FRET or coimmunoprecipitation experiments, indicated a significant interaction between TRPV1 and TRPV3 in our hands. As both studies applied HEK293 cells as the expression system, it remains to be determined whether the species differences of the investigated TRPV channel isotypes can account for the discrepancies.

The rules governing subunit assembly and, in particular, protein domains that provide specific interaction between TRPV channel subunits remain to be determined. Detailed information concerning cytosolic protein domains that mediate assembly of hexahelical cation channels is available for potassium channels and for cyclic nucleotide-gated channels (Li et al., 1994; Liu et al., 1996; Zhong et al., 2002). The hydrophilic N-termini of Shaker K^+ channel subunits (referred to as the T1 domain) are sufficient to form tetrameric complexes (Li et al., 1992; Pfaffinger and DeRubeis, 1995; Kreusch et al., 1998). For CNG and HCN channels however, a tetramerization domain has been localized to the cytosolic C-terminus (Zagotta et al., 2003; Zhong et al., 2002). In addition, a direct interaction between HCN1 and HCN2 can be mediated by their N-termini (Proenza et al., 2002). Our data are compatible with a significant contribution of the cytosolic N-terminus to the assembly of TRPV4 subunits. These data are in agreement with those describing a specific interaction between ankyrin-like repeats located in the N-terminus of TRPV6 (Erler et al., 2004).

In contrast to TRPV4, the N-terminus of TRPV1 neither confers a strong homophilic interaction nor does it associate with full-length TRPV1 subunits. Although we confirm the homophilic interaction of the TRPV1 C-terminus (García-Sanz et al., 2004), its overall contribution to TRPV1 channel assembly appears limited as assessed by the interaction between chimeric TRPV channel constructs and by the lack of a dominant-negative effect on TRPV1 function. In contrast, our data suggest that TRPV1 subunits predominantly assemble through an interaction of protein moieties located between transmembrane segments 1-6. Similar findings, but with additional stabilization in the N-terminus have been reported for the interaction between transmembrane domains of *Drosophila* TRP (Xu et al., 1997). In agreement with the recent finding (Chang et al., 2004) that TRPV5 assembly requires interaction of both N- and C-termini, we conclude that TRPV

channel assembly is determined by more than one site of interaction. Both cytosolic termini and transmembrane segments synergistically contribute to the overall affinity between TRPV channel subunits and control the selectivity of homo- and heteromeric assembly of the pore-forming TRPV subunits. The relative contribution of cytoplasmic and intramembrane binding modules presumably differs between the TRPV channel isoforms. Thus, in addition to previous studies, we demonstrate that the inter-subunit interaction between TRPV subunits also involves the transmembrane portion of the protein. This may be not unexpected because parts of hexahelical channel subunits that are flanking the pore probably come into close contact with their transmembrane segments 5 and 6 and also their pore loops (Roux and MacKinnon, 1999) to stabilize the closed pore conformation of the inactive channel complex or to maintain the selectivity filter upon gating.

Having studied the heteromer formation in the TRPC and TRPV channel families consisting of six to seven members each, it is tempting to draw preliminary conclusions about the rules of random versus evolutionarily favored maintenance of heteromeric subunit interaction. During phylogenesis, gene duplications represent the branching points at which two almost identical proteins form and subsequently diverge by individually accumulating mutations. At a certain level of divergence, either the heteromultimerization will be lost or co-evolution between two subunits will help maintain or even create complementary binding interfaces. Although, theoretically, only a few amino acid exchanges may suffice to disrupt the inter-subunit interaction, a multi-step procedure for creating two independently assembling cation channel complexes is more likely. The TRPC channel family can be subdivided into two major subgroups: TRPC1, TRPC4 and TRPC5 sharing 40-68% amino acid identity, or TRPC3, TRPC6 and TRPC7 featuring >72-79% amino acid identity. Within the mammalian TRPV and TRPC channel families, the highest amino acid identity between non-interacting subunits is 41.4% for TRPV1 and TRPV4 whereas the lowest identity of interacting partners is 40.5% for TRPC1 and TRPC4. Thus, intriguingly, the threshold for the phylogenetic conservation of heteromultimerization between mammalian TRPC or TRPV channel subunits appears to be tightly defined. In contrast to the TRPV and TRPC channel families, CNG channel complexes are composed of A-type and B-type subunits (Weitz et al., 2002; Zheng et al., 2002). Because the overall amino acid sequence identity between interacting CNGA1-4 and CNGB1/3 channel subunits amounts to only 16-32% (Kaupp and Seifert, 2002), it is likely that co-evolution of the binding interfaces occurred. In the TRP channel family and on the basis of currently available data, such signs of co-evolution are limited and may be restricted to the eye-specific insect TRP, TRPL and TRP-γ channels, which share 37-38% amino acid identity, but still form heteromeric complexes (Xu et al., 1998; Xu et al., 2002). Because the overall amino acid identity between cation channel subunits does not necessarily reflect local similarities in the binding interface(s), a more refined analysis of the binding determinants will help clarify the validity of these initial thoughts.

In conclusion, our data demonstrate that, except for TRPV5 and TRPV6, TRPV channel subunits preferentially assemble into homomeric pore complexes. Although in the presence of as yet unidentified accessory subunits the TRPV heteromultimerization may be altered, we describe here the intrinsic properties of the pore-forming TRPV subunits to assemble into homo- or hetero-oligomeric channel complexes. The overall affinity and the specificity of interaction appear to be synergistically defined by both transmembrane domains and cytosolic termini, presumably by forming intramolecularly linked interaction modules.

We thank Robert Kraft for confirming the functional integrity of TRPV5-YFP and TRPV6-YFP clones by electrophysiological recordings. This work was supported by the Deutsche Forschungsgemeinschaft and by the Fonds der Chemischen Industrie.

References

Amiri, H., Schultz, G. and Schaefer, M. (2003). FRET-based analysis of TRPC subunit stoichiometry. *Cell Calcium* **33**, 463-470.

Bichet, D., Haass, F. A. and Jan, L. Y. (2003). Merging functional studies with structures of inward-rectifier K^+ channels. *Nature* **4**, 957-967.

Birder, L. A., Nakamura, Y., Kiss, S., Nealen, M. L., Barrick, S., Kanai, A. J., Wang, E., Ruiz, G., de Groat, W. C., Apodaca, G. et al. (2002). Altered urinary bladder function in mice lacking the vanilloid receptor TRPV1. *Nat. Neurosci.* **5**, 856-860.

Boels, K., Glassmeier, G., Herrman, D., Riedels, I. B., Hampe, W., Kojima, I., Schwarz, J. R. and Schaller, H. C. (2001). The neuropeptide head activator induces activation and translocation of the growth-factor-regulated Ca^{2+}-permeable channel GRC. *J. Cell Sci.* **114**, 3599-3606.

Caterina, M. J., Schumacher, M. A., Tominaga, M., Rosen, T. A., Levine, J. D. and Julius, D. (1997). The capsaicin receptor: a heat-activated ion channel in the pain pathway. *Nature* **389**, 816-824.

Caterina, M. J., Rosen, T. A., Tominaga, M., Brake, A. J. and Julius, D. (1999). A capsaicin-receptor homologue with a high threshold for noxious heat. *Nature* **398**, 436-441.

Chang, Q., Gyftogianni, E., van de Graaf, S. F., Hoefs, S., Weidema, F. A., Bindels, R. J. and Hoenderop, J. G. (2004). Molecular determinants in TRPV5 channel assembly. *J. Biol. Chem.* **279**, 54304-54311.

Chung, M. K., Lee, H. and Caterina, M. J. (2003). Warm temperatures activate TRPV4 in mouse 308 keratinocytes. *J. Biol. Chem.* **278**, 32037-32046.

Cui, J., Bian, J. S., Kagan, A. and McDonald, T. V. (2002). CaT1 contributes to the store-operated calcium current in Jurkat T-lymphocytes. *J. Biol. Chem.* **277**, 47175-47183.

den Dekker, E., Hoenderop, J. G., Nilius, B. and Bindels, R. J. (2003). The epithelial calcium channels, TRPV5 & TRPV6: from identification towards regulation. *Cell Calcium* **33**, 497-507.

Erler, I., Hirnet, D., Wissenbach, U., Flockerzi, V. and Niemeyer, B. A. (2004). Ca^{2+}-selective transient receptor potential V channel architecture and function require a specific ankyrin repeat. *J. Biol. Chem.* **279**, 34456-34463.

Eun, S. Y., Jung, S. J., Park, Y. K., Kwak, J., Kim, S. J. and Kim, J. (2001). Effects of capsaicin on Ca^{2+} release from the intracellular Ca^{2+} stores in the dorsal root ganglion cells of adult rats. *Biochem. Biophys. Res. Commun.* **285**, 1114-1120.

García-Sanz, N., Fernández-Carvajal, A., Morenilla-Palao, C., Planells-Cases, R., Fajardo-Sánchez, E., Fernández-Ballester, G. and Ferrer-Montiel, A. (2004). Identification of a tetramerization domain in the C terminus of the vanilloid receptor. *J. Neurosci.* **24**, 5307-5314.

Goel, M., Sinkins, W. G. and Schilling, W. P. (2002). Selective association of TRPC channel subunits in rat brain synaptosomes. *J. Biol. Chem.* **277**, 48303-48310.

Gunthorpe, M. J., Benham, C. D., Randall, A. and Davis, J. B. (2002). The diversity in the vanilloid (TRPV) receptor family of ion channels. *Trends Pharmacol. Sci.* **23**, 183-191.

Hellwig, N., Plant, T. D., Janson, W., Schäfer, M., Schultz, G. and Schaefer, M. (2004). TRPV1 acts as proton channel to induce acidification in nociceptive neurons. *J. Biol. Chem.* **279**, 34553-34561.

Hoenderop, J. G., van der Kemp, A. W., Hartog, A., van de Graaf, S. F., van Os, C. H., Willems, P. H. and Bindels, R. J. (1999). Molecular Identification of the apical Ca^{2+} channel in 1,25-dihydroxyvitamin D_3-responive epithelia. *J. Biol. Chem.* **274**, 8375-8378.

Hoenderop, J. G., Voets, T., Hoefs, S., Weidema, F., Prenen, J., Nilius, B. and Bindels, R. J. (2003). Homo- and heterotetrameric architecture of the epithelial Ca^{2+} channels TRPV5 and TRPV6. *EMBO J.* **22**, 776-785.

Hofmann, T., Schaefer, M., Schultz, G. and Gudermann, T. (2002). Subunit composition of mammalian transient receptor potential channels in living cells. *Proc. Natl. Acad. Sci. USA* **99**, 7461-7466.

Kanzaki, M., Zhang, Y. Q., Mashima, H., Lu, L., Shibata, H. and Kojima, I. (1999). Translocation of a calcium-permeable cation channel induced by insulin-like growth factor-I. *Nature* **1**, 165-170.

Kaupp, U. B. and Seifert, R. (2002). Cyclic nucleotide-gated ion channels. *Physiol. Rev.* **82**, 769-824.

Kedei, N., Szabo, T., Lile, J. D., Treanor, J. J., Olah, Z., Iadarola, M. J. and Blumberg, P. M. (2001). Analysis of the native quaternary structure of vanilloid receptor 1. *J. Biol. Chem.* **276**, 28613-28619.

Kreusch, A., Pfaffinger, P. J., Stevens, C. F. and Choe, S. (1998). Crystal structure of the tetramerization domain of the *Shaker* potassium channel. *Nature* **392**, 945-948.

Lenz, J. C., Reusch, H. P., Albrecht, N., Schultz, G. and Schaefer, M. (2002). Ca^{2+}-controlled competitive diacylglycerol binding of protein kinase C isoenzymes in living cells. *J. Cell Biol.* **159**, 291-301.

Li, M., Jan, Y. N. and Jan, L. Y. (1992). Specification of subunit assembly by the hydrophilic amino-terminal domain of the Shaker potassium channel. *Science* **257**, 1225-1230.

Li, M., Unwin, N., Stauffer, K. A., Jan, Y. N. and Jan, L. Y. (1994). Images of purified Shaker potassium channels. *Curr. Biol.* **4**, 110-115.

Liu, D. T., Tibbs, G. R. and Siegelbaum, S. A. (1996). Subunit stoichiometry of cyclic nucleotide-gated channels and effects of subunit order on channel function. *Neuron* **16**, 983-990.

Liu, M., Liu, M. C., Magoulas, C., Priestley, J. V. and Willmott, N. (2003). Versatile regulation of cytosolic Ca^{2+} by vanilloid receptor I in rat dorsal root ganglion neurons. *J. Biol. Chem.* **278**, 5462-5472.

Marshall, I. C., Owen, D. E., Cripps, T. V., Davis, J. B., McNulty, S. and Smart, D. (2003). Activation of vanilloid receptor 1 by resiniferatoxin mobilizes calcium from inositol 1,4,5-trisphosphate-sensitive stores. *Br. J. Pharmacol.* **138**, 172-176.

Olah, Z., Szabo, T., Karai, L., Hough, C., Fields, R. D., Caudle, R. M., Blumberg, P. M. and Iadarola, M. J. (2001). Ligand-induced dynamic membrane changes and cell deletion conferred by vanilloid receptor 1. *J. Biol. Chem.* **276**, 11021-11030.

Peng, J. B., Chen, X. Z., Berger, U. V., Vassilev, P. M., Tsukaguchi, H., Brown, E. M. and Hediger, M. A. (1999). Molecular cloning and characterization of a channel-like transporter mediating intestinal calcium absorption. *J. Biol. Chem.* **274**, 22739-22746.

Peng, J. B., Brown, E. M. and Hediger, M. A. (2001). Structural conservation of the genes encoding CaT1, CaT2, and related cation channels. *Genomics* **76**, 99-109.

Pfaffinger, P. J. and DeRubeis, D. (1995). Shaker K^+ channel T1 domain self-tetramerizes to a stable structure. *J. Biol. Chem.* **270**, 28595-28600.

Proenza, C., Tran, N., Angoli, D., Zahynacz, K., Balcar, P. and Accili, E. A. (2002). Different roles for the cyclic nucleotide binding domain and amino terminus in assembly and expression of hyperpolarization-activated, cyclic nucleotide-gated channels. *J. Biol. Chem.* **277**, 29634-29642.

Robinson, R. B. and Siegelbaum, S. A. (2003). Hyperpolarization-activated cation currents: from molecules to physiological functions. *Annu. Rev. Physiol.* **65**, 453-480.

Roosild, T. P., Lê, K. T. and Choe, S. (2004). Cytoplasmic gatekeepers of K^+-channel flux: a structural perspective. *Trends Biochem. Sci.* **29**, 39-45.

Roux, B. and MacKinnon, R. (1999). The cavity and pore helices in the KcsA K^+ channel: electrostatic stabilization of monovalent cation. *Science* **285**, 100-102.

Schaefer, M., Albrecht, N., Hofmann, T., Gudermann, T. and Schultz, G. (2001). Diffusion-limited translocation mechanism of protein kinase C isotypes. *FASEB J.* **15**,1634-1636.

Schaefer, M., Plant, T. D., Obukhov, A. G., Hofmann, T., Gudermann, T. and Schultz, G. (2000). Receptor-mediated regulation of the nonselective cation channels TRPC4 and TRPC5. *J. Biol. Chem.* **275**, 17517-17526.

Smith, G. D., Gunthorpe, M. J., Kelsell, R. E., Hayes, P. D., Reilly, P., Facer, P., Wright, J. E., Jerman, J. C., Walhin, J. P., Ooi, L. et al. (2002). TRPV3 is a temperature-sensitive vanilloid receptor-like protein. *Nature* **418**, 186-190.

Strotmann, R., Harteneck, C., Nunnenmacher, K., Schultz, G. and Plant, T. D. (2000). oTRPC4, a nonselective cation channel that confers sensitivity to extracellular osmolarity. *Nat. Cell Biol.* **2**, 695-702.

Strübing, C., Krapivinsky, G., Krapivinsky, L. and Clapham, D. E. (2001). TRPC1 and TRPC5 form a novel cation channel in mammalian brain. *Neuron* **29**, 645-655.

Tominaga, M., Caterina, M. J., Malmberg, A. B., Rosen, T. A., Gilbert, H., Skinner, K., Raumann, B. E., Basbaum, A. I. and Julius, D. (1998). The cloned capsaicin receptor integrates multiple pain-producing stimuli. *Neuron* **21**, 531-543.

Vennekens, R., Hoenderop, J. G., Prenen, J., Struiver, M., Willems, P. H., Droogmans, G., Nilius, B. and Bindels, R. J. (2000). Permeation and gating properties of the novel epithelial Ca^{2+} channel. *J. Biol. Chem.* **275**, 3963-3969.

Vriens, J., Watanabe, H., Janssens, A., Droogmans, G., Voets, T. and Nilius, B. (2004). Cell swelling, heat, and chemical agonists use dinstinct pathways for the activation of the cation channel TRPV4. *Proc. Natl. Acad. Sci. USA* **101**, 396-401.

Watanabe, H., Davis, J. B., Smart, D., Jerman, J. C., Smith, G. D., Hayes, P., Vriens, J., Cairns, W., Wissenbach, U., Prenen, J. et al. (2002a). Activation of TRPV4 channels (hVRL-2/mTRP12) by phorbol derivates. *J. Biol. Chem.* **277**, 13569-13577.

Watanabe, H., Vriens, J., Suh, S. H., Benham, C. D., Droogmans, G. and Nilius, B. (2002b). Heat-evoked activation of TRPV4 channels in a HEK293 cell expression system and in native mouse aorta endothelial cells. *J. Biol. Chem.* **277**, 47044-47051.

Weitz, D., Ficek, N., Kremmer, E., Bauer, P. J. and Kaupp, U. B. (2002). Subunit stoichiometry of the CNG channel of rod photoreceptors. *Neuron* **36**, 881-889.

Xu, F., Satoh, E. and Iijima, T. (2003). Protein kinase C-mediated Ca^{2+} entry in HEK 293 cells transiently expressing human TRPV4. *Br. J. Pharmacol.* **140**, 413-421.

Xu, X. Z., Li, H. S., Guggino, W. B. and Montell, C. (1997). Coassembly of TRP and TRPL produces a distinct store-operated conductance. *Cell* **89**, 1155-1164.

Xu, X. Z., Chien, F., Butler, A., Salkoff, L. and Montell, C. (2000). TRPγ, a *Drosophila* TRP-related subunit, forms a regulated cation channel with TRPL. *Neuron* **26**, 647-657.

Zagotta, W. N., Olivier, N. B., Black, K. D., Young, E. C., Olson, R. and Gouaux, E. (2003). Structural basis for modulation and agonist specificity of HCN pacemaker channels. *Nature* **425**, 200-205.

Zheng, J., Trudeau, M. C. and Zagotta, W. N. (2002). Rod cyclic nucleotide-gated channels have a stoichiometry of three CNGA1 subunits and one CNGB1 subunit. *Neuron* **36**, 891-896.

Zhong, H., Molday, L. L., Molday, R. S. and Yau, K. W. (2002). The heteromeric cyclic nucleotide-gated channel adopts a 3A:1B stoichiometry. *Nature* **420**, 193-198.